INTERNATIONAL JOURNAL OF
COASTAL & OFFSHORE ENGINEERING
IJCOE Vol.5/No. 4/Winter 2020 (35-46)

Available online at: www. Ijcoe.org

Experimental Performance Evaluation of a Hydraulic PTO System for Centipede Wave Energy Converter

Mozhgan Aghanezhad [1], Rouzbeh Shafaghat [2*], Rezvan Alamian[3]

[1] *MSc Student, Sea-Based Energy Research group, Babol Noshirvani University of Technology; mozhganaghanezhad@nit.ac.ir*
[2*] *Associated Professor, Sea-Based Energy Research group, Babol Noshirvani University of Technology; rshafaghat@nit.ac.ir*
[3] *Senior Research Associate, Sea-Based Energy Research group, Babol Noshirvani University of Technology; ralamian@nit.ac.ir*

ARTICLE INFO

Article History:
Received: 16 Jun. 2020
Accepted: 08 Sep. 2020

Keywords:
Marine Energy
Centipede Wave Energy Converter
Hydraulic PTO
Experimental Analysis
Optimization

ABSTRACT

In the past decade, ocean and marine waves like other renewable energy sources attracted attention due to its high energy density. The most important part of a wave energy converter (WEC) is power take-off (PTO) system. In this study, a proper hydraulic power take-off system for centipede WECs has been evaluated and analyzed in experimental scale. Experimental analysis has been done in dry conditions. Important parameters are resistant load of rheostats and the opening percent of the flow control valve. System input is the wave force, which is modeled as an external mechanical force applied to the end of the lever. Resistant load of rheostats is changeable in the range of 9.5 to 55 ohms. In addition, according to the range of valve opening, six positions are selected to study. Results in this research show that, as resistance load increases, output power and efficiency, are enhanced significantly. On the other hand, in all the resistive loads tested, there is a maximum point (2 rev. valve opening) for efficiency, which shows the positive effect of controlling the input flow to the Hydro Motor (HM). The efficiency in this position of the flow control valve opening has enhanced by 40% compared to neighbor situations.

1. Introduction

Nowadays, human lifestyle and living standards have been changed. Besides, increasing energy consumption in all aspects of life is a force to use more and more energy. Oil crisis, reducing fossil resources, and increasing global warming have led human thought to use renewable resources, re-produced every day. Among them, utilization of natural sources like sun, wind, water and ocean are on top. Likewise, international treaties as Paris Agreement and Kyoto Protocol are motivation and encourage for activists in this context [1-3]. It is worth noting that extracting marine energy as a major and promising source, with having more available energy potential (between 15 to 20 times more) than wind or solar energy, has inspired enormous interest [4].

A brief insight into geographical situation of Iran, indicates more than 20% of the population, business centers, recreation centers and residential areas are focused near 2700 km shoreline of Iran [5]. Therefore, strategic attention to different types of harnessing wave energy is very important for generating electrical power. In this regard, Caspian Sea as the largest lake in the world, despite being closed compared to other open waters, has a great potential of extracting energy due to its continuous waves [6].

Wave energy converter is one of the latest technology in the world, produce energy from ocean and seas. The requirement for such projects to be economical is the definition and implementation of coherent research projects in laboratory and semi-industrial dimensions, in order to evaluate the system and the parameters affecting it. Over the past decades, a wide variety of WECs have been developed and can be said: hundreds of prototypes have been registered to extract wave energy so far. In general WECs can be classified according to three characteristics: location (onshore, nearshore and offshore), size (point absorber, terminator and attenuator) and working principle (overtopping, pressure differential, impact and floating structure) [3].

In order to utilize the WECs, lots of researches has spurred. In 2007 Waters et al. have studied a full scale prototype of a point absorber WEC in the Swedish west

coast [7]. Tests have been done for different wave climate. It has been indicated that, for resistive loads, optimal load is existed. Many researches have been done to study different shapes of buoys. Sarlak et al. optimized the buoy configuration in heave and pitch mode [8]. Yousefi et al. in 2016 examined the Wavestar WEC under the Caspian Sea parameters. They studied parameters such as arm length, buoy dimension, wave period and wave height [6]. An experimental study has investigated on the Centipede WEC of attenuator type, with 6 spherical buoys by Alamian et al. in 2019 [4]. This study has been done in the wave tank of the Babol Noshirvani University of Technology and main parameters were amplitude and period of different sea waves.

One of the most important parts of any wave energy converter is the power take-off system. In this regard, the fundamental issue in the operation of WECs is controlling PTO to achieve optimum energy from waves. This has massive impact on maximizing the WEC utilization; especially on large scale wave power plants. Henderson in 2006 applied active control for PTO to maximize power capture across a range of sea-states and improve survivability [9]. Drew et al. in 2009 introduced the state of WEC technology at the time, established different device types, classified PTO systems and considered some of the control strategies to enhance the efficiency of point absorber-type WECs [10]. In 2014, Hansen et al. developed a new PTO based on discrete hydraulics (using multi-chambered cylinders) named as Discrete Displacement Cylinder (DDC); to improve the power production of the 1 MW wave energy converter, Wavestar [11]. Nguyen et al. in 2016 showed the high potential of improvement brought by Model Predicting Control (MPC) in terms of harvested power [12].

In spite of substantial impact of applying control system to PTO on power quality and quantity (Lopes et al. in 2009 [13] and Kramer et al. in 2011 [14]), the adjustments of PTO system components is also very important. Accordingly, optimized power extraction can be achieved by defining proper resistant load, input fluid flow limitation to HM and specific input condition in hydraulic PTO system. In this research, performance of WEC is evaluated; considering flow control valve opening and resistant load (in electrical circuit) as important parameters. For quantitative analysis, output power (watts) and more importantly, total efficiency of the system are analyzed. Other parameters like HM pressure difference, rotational velocity of coupled HM and generator shaft, voltage and current are recording by camera (Nikon, L830).

According to the defined goals, in order to describe the problem first, the desired power take-off system is introduced; then in research method section, laboratory equipment, test method, and how to process the output data are considered. In the following, system efficiency is analyzed and results are presented. In the conclusion section, the most important results are explained.

2. Problem Definition

2.1. Power take-off system

The desired hydraulic power take-off system is designed for Centipede WEC (namely IRWEC2). The first step in developing process was done successfully in the form of experimental investigation at Sea-Based Energy Research Group of Babol Noshirvani University of Technology (Figure 1) [4]. In this laboratory model, mechanical power take-off system was used. Two configurations including 6 and 10 buoys were tested in several wave amplitudes and wave periods, and output power were surveyed [4].

(a)

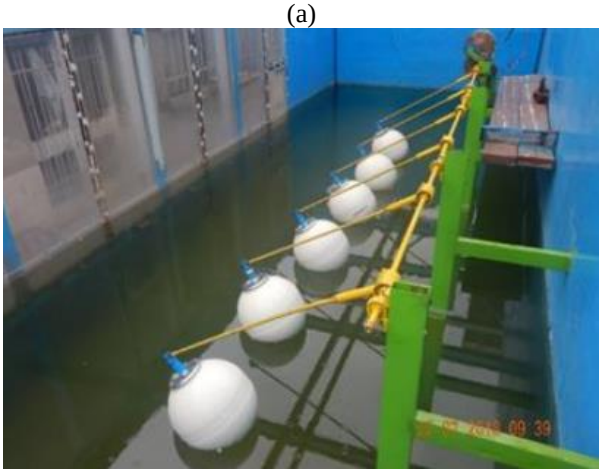

(b)

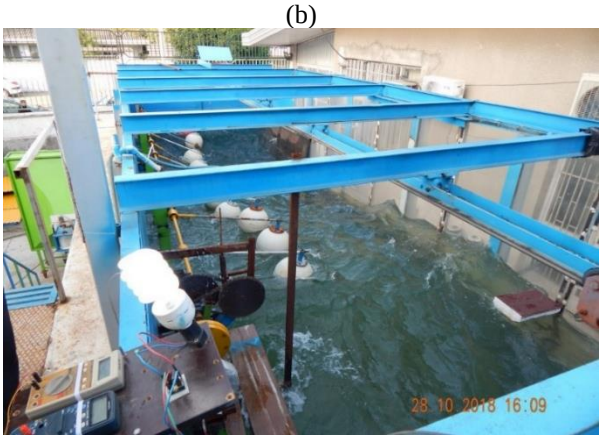

Figure 1. Centipede WEC that was built and tested in Sea-Based Energy Research Group of Babol Noshirvani University of Technology with mechanical PTO system; (a): 6 arms centipede WEC, (b): 10 arms centipede WEC

In the second step of developing process in larger scale, for extracting more power, a hydraulic power take-off system is chosen due to its well adapted characteristics to sea waves (large forces at low frequencies). Schematic plan of hydraulic PTO system in IRWEC2 is shown in Figure 2 In this study, before launching the WEC to wave tank, dry tests are implemented on hydraulic PTO outside the wave tank. The ultimate goal is parametric evaluation and achievement of appropriate operation points for PTO system.

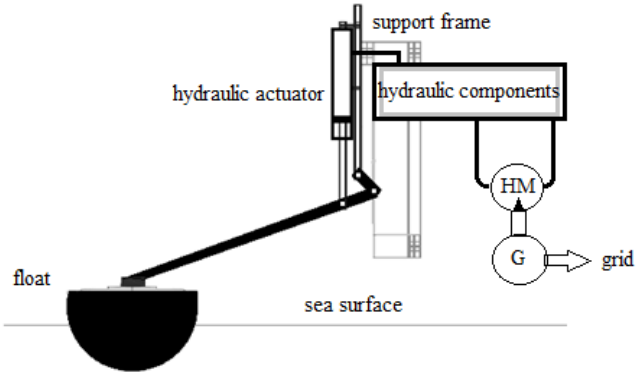

Figure 2. General schematic of Centipede WEC with hydraulic PTO system

2.2. Caspian Sea Waves

Before installing PTO system on WEC, ensuring of optimal system performance according to wave characteristics of the target sea is very important. As the WEC is developed to operate in the Caspian Sea, experimental wave modeling in laboratory is based on its wave condition. Figure 3 illustrates time-averaged wave energy per unit length of the wave front for mean wave period and significant wave height of the Caspian Sea near the Babolsar. The color scale represents total annual energy per unit length of wave front, the bold numbers indicate the occurrence of sea states in number of hours per year.

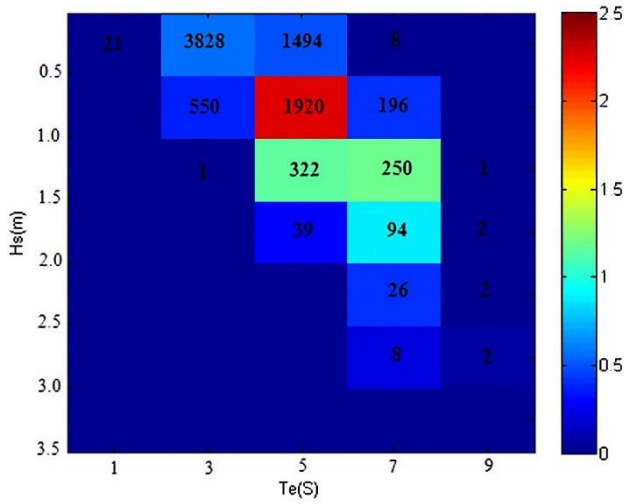

Figure 3. Combined scatter and energy diagrams of the annual energy corresponding to sea states in different ranges of Hs and Te for Caspian Sea (near Babolsar) [15]

As can be seen in this figure, significant wave height (Hs) within the ranges of 0.5 to 1 m and mean wave period (Te) between 4 and 6 s, satisfies both maximum energy and occurrences. Therefore, the significant wave height of 70 cm is selected for evaluating the WEC. Regarding to wave period; as period decreases, force applied to WEC increases and critical condition may occur. Therefore 2 seconds wave period can be considered.

3. Research Method

3.1. Laboratory Equipment

As shown in Figure 2, hemisphere buoy is connected to the support frame and hydraulic actuator by an arm. To investigate dry tests, in the absence of buoy, equivalent force is applied to the lever (110 cm arm in Figure 4-a). Transmission mechanism is 4-bar linkage (Figure 4-b, c). Sinusoidal input wave moves the buoy in heave direction and activates the hydraulic actuator. Hydraulic cylinder has a stroke of 245 (mm), but according to test requirements, 12 (cm) displacement is sufficient. Hydraulic actuator along with other existing components provide a certain pressure difference for HM. Output rotational motion of the HM, by coupling to the generator produces electricity. Figure 5 depicts P&ID diagram for hydraulic PTO system and related equipment.

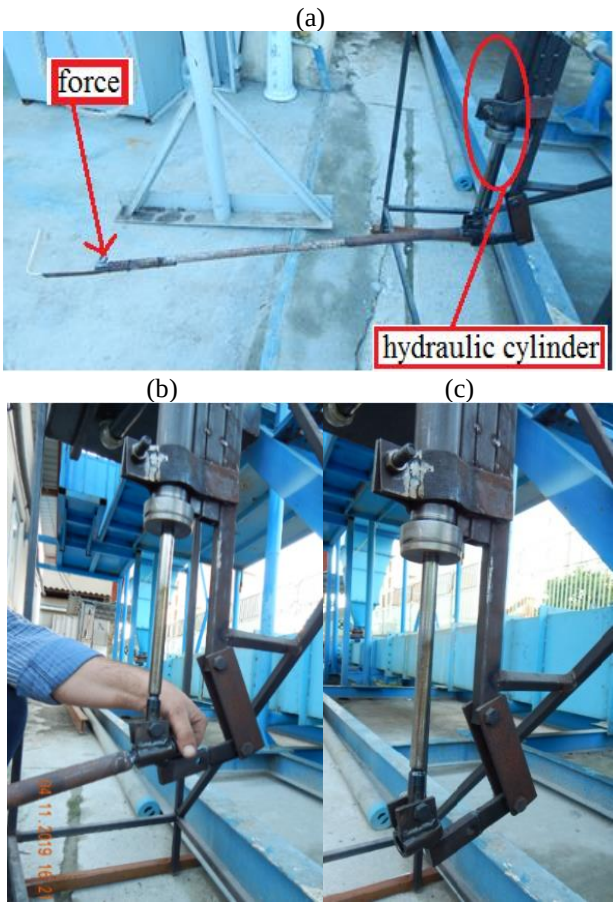

Figure 4. Lever and piston motion mechanisms of WEC

Final set-up for testing hydraulic PTO is illustrated in Figure 6. It's noteworthy that a 50 liters capacity oil tank is used for keeping, purify and cooling the circulating oil. Circulating oil is a hydraulic oil named HLP 51524 part 2. Used hydraulic actuator is a single-acting hydraulic cylinder and 2 check valves are used on both sides of the cylinder to prevent back flow.

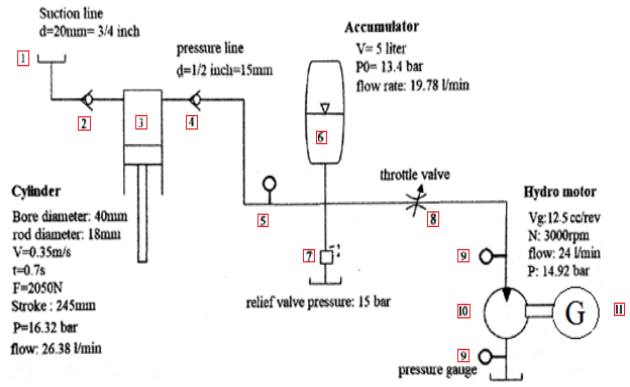

Figure 5. Schematic of hydraulic circuit and components

Figure 6. Test setup for centipede WEC

An accumulator is used to prevent oscillations and regulate system pressure. By locating a flow control valve before HM, input flow rate (velocity) is controlled. A relief valve is installed after the accumulator and before the flow control valve to prevent undesirable increase in pressure and to protect the pressure-sensitive parts and equipment. The pressure is relieved by allowing the pressurized fluid to flow from an auxiliary passage out of the system, when necessary. To measure the pressure, there are 3 pressure gauges in hydraulic circuit; one in charge line and two of them are on both input and output flow of the HM. HM is a gerotor (inner gear motor) type motor with 12.5 cc displacement. A brief technical information on mentioned equipment are pointed out in Table 1.

Table 1. Technical information of setup components.

	name	Technical information	accuracy
1	Oil tank	Tank capacity: 50 liter	-
2	Check valve	A one-way spring-ball valve (3/4 in), between oil tank and cylinder	-
3	Hydraulic cylinder	Single-acting cylinder, 18 mm rod diameter, 245 mm displacement	-
4	Check valve	A one-way spring-ball valve (1/2 in), between cylinder and accumulator	-
5	Pressure gauge	Liquid filled 40 bar gauge	±0.5%
6	Accumulator	5 liter capacity	-
7	Relief valve	Pressure relief valve se at 15 bar	-
8	Control valve	Needle valve	-
9	Pressure gauge	Liquid filled 25 bar gauge	±0.5%
10	Hydro motor	12.5 cc gerotor	-
11	Generator	Axial-Flux Permanent Magnets Generator (AFPMG) TGET260-I-0.1KW	-
12	Hydraulic oil	HLP 51524 part 2	-
13	Multi meter	HIOKI 3256-DIGITAL Hi TESTER	±0.6%
14	Multi meter	HIOKI 3200- DIGITAL Hi TESTER	±1.5%
15	Force gauge	Radex force gauge	±0.05%
16	Tachometer	Lutron tachometer DT-2268 (contact-laser)	±0.05%

As mentioned before, in the absence of buoy, for modeling its motion, applying a sinusoidal mechanical force (excitation force for cylinder) to the end of arm can move the hydraulic cylinder. According to Figure 7, the force is applied to the end of lever (arm) by rope and pulley system. In addition, this force is measured by a digital force gauge.

The generator coupled to HM is an Axial-Flux Permanent Magnets Generator (Figure 8). As figure shows, a rheostat is used to apply resistant load. Also, the electric current passing through the rheostat and its voltage are measured by two multimeters. Output data from the measurement equipment (tachometer, pressure gauges, rheostat and multimeters) is recorded by a camera for subsequent analysis. It should be noted that the output current of generator is three-phase at first; the three-phase output is rectified by a bridge rectifier (Figure 9).

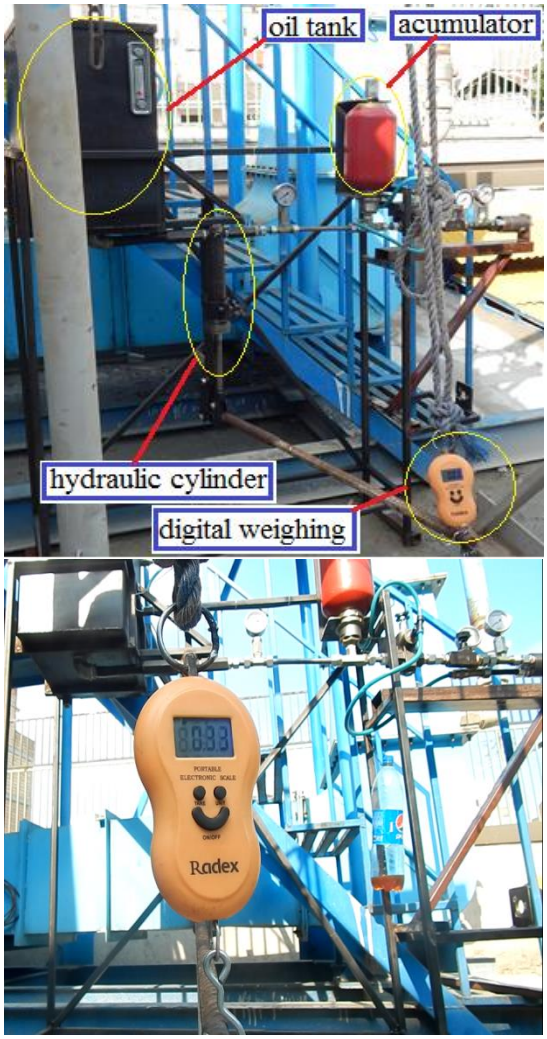

Figure 7. Mechanical force measurement in hydraulic PTO system

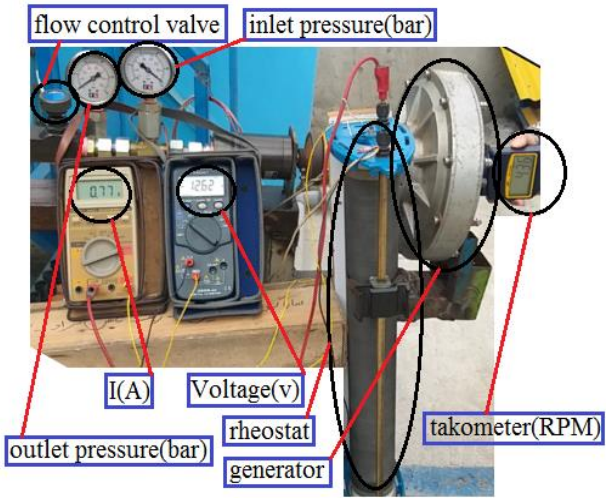

Figure 8. Set-up of measuring instruments

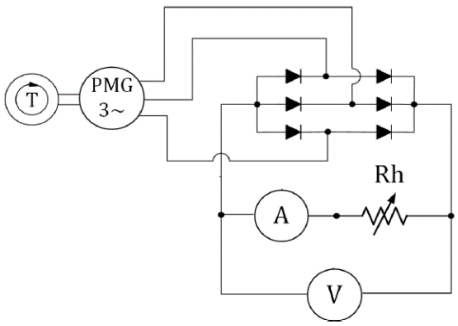

Figure 9. Electric circuit including Diode Bridge (bridge rectifier), rheostat and voltage and current measurement elements

3.2. Test procedure

As mentioned earlier, in order to perform experimental tests, it is important to pay attention to two parameters, the amount of opening of the flow control valve and the amount of load applied by the rheostat. Flow control valve has a manual regulator that is opened in the range of [0.5 to 3] revolution with the step of 0.5 rev. (Figure 10). For exact adjustment of the control valve opening in the defined modes, the control valve body and also the valve is marked at fully closed stage (Figure 10-a). In Figures 10-b and 10-c, valve opening process is depicted clearly.

(a)

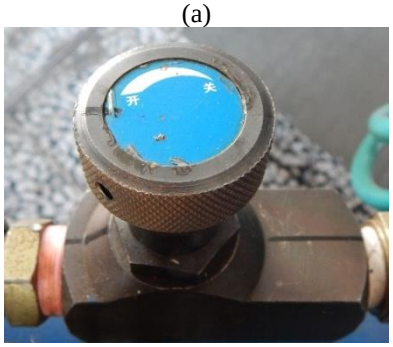

(b)

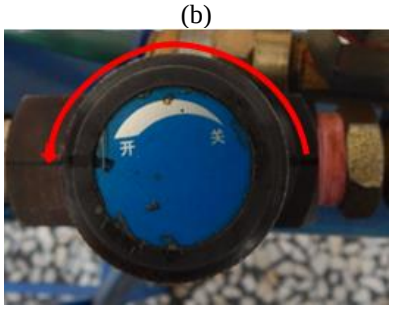

(c)

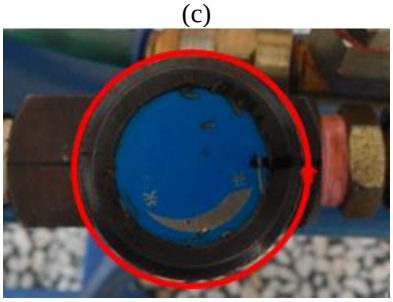

Figure 10. Flow control valve and related settings for opening positions

Continuity in HM output shaft is of high importance; thus in fully closed fluid path (closed control valve) by applying mechanical force to lever, both accumulator charging and pressure difference can be provided (for HM). After the accumulator has been charged, hydraulic fluid flows through the HM. In this status; by applying continues mechanical force to lever, continues rotation of HM and then generator is enabled. As it is clear in Figure 6, three pressure gauges are installed in hydraulic path. The first one is before accumulator that measures its pressure. The second and the third one are before and after he HM, respectively. At first, input path for hydraulic oil is closed, then mechanical force increases the line pressure. At this time, the application of mechanical force continues until the line pressure (first gauge) reaches 30 bar and accumulator is charged. Hence, the fear of pressure drop during testing or data collection reduces. If the pressure is reduced, the mechanical force will be compensated by continuing to apply force to the lever. At this stage, after opening the control valve, pressure increases suddenly in second gauge. Then by rotating common shaft of HM and generator, power production initiates. Discharging hydraulic oil passing the third gauge, returns to oil tank. The third gauge shows the pressure of discharging hydraulic fluid that almost all the time is zero; means the HM converts all the fluid pressure to work. Contemplative point is fluid pressure loss in the hydraulic circuit. Experiments have shown that maximum pressure difference value between first and second gauges is about 1 bar; but significant pressure difference is before and after the HM. As a result, the most dissipation (power transmission) is observed at this zone.

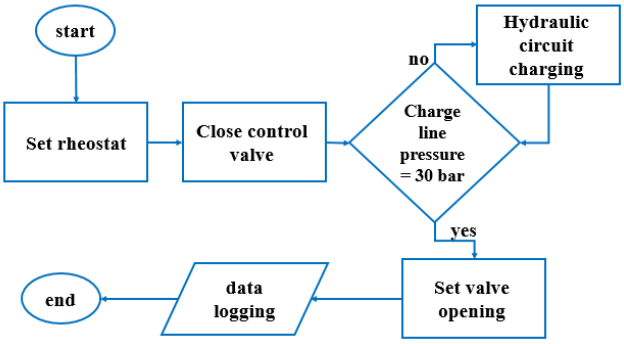

Figure 11. Test flowchart

In each mode of control valve, load of rheostat changes in the range [0 -55] ohms; exactly are set on values of 9.5, 22, 34, 39, 44.5, 50, and 54.8 ohms. Output data in this stage are voltage and current, measured by a pair of multi meters. In addition, for detailed study, force gauge measures the applied force, when lever goes up to the end of its course (in half of the modeled wave period). Therefore, the lever returns to its initial position under the influence of weight and the mechanical force is zero. Procedure of the test is shown in form of a flowchart in Figure 11.

4. Output data processing

4.1. Mechanical force

One of the measured parameters is mechanical force. Due to the lever motion type, quadratic polynomial interpolation is used for the obtained data (Figure 12). Measured force in different modes of control valve is provided in Figure 13. A common point in all situation is measured force convergence to constant value. This constant value of mechanical force is used for calculation. Also, due to the slight difference in the data of the interpolation polynomial and the measured data, the values of the interpolation polynomial are used in the calculations.

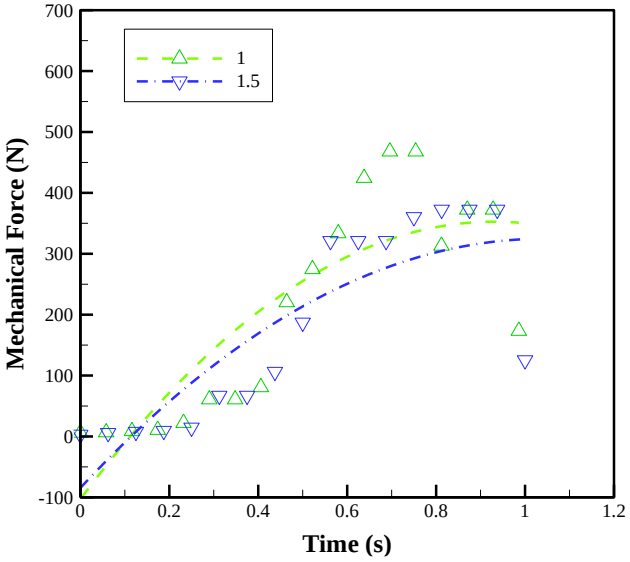

Figure 12. Applied mechanical force diagrams in 1 and 1.5 rev positions and related quadratic curve fitting

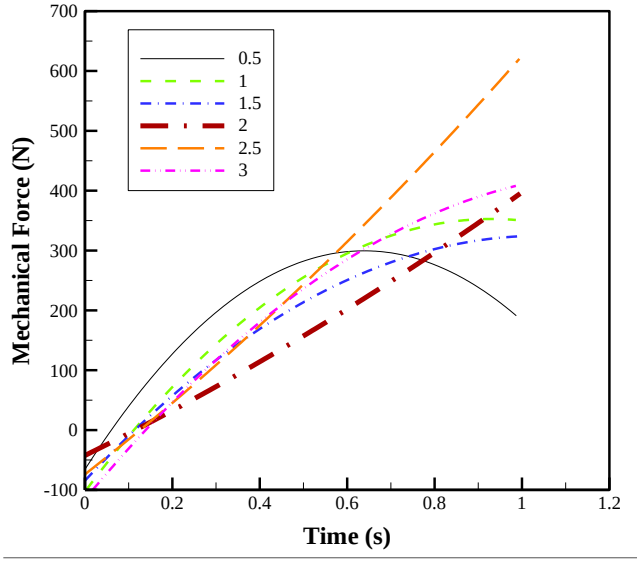

Figure 13. Applied mechanical force curves in all valve positions

By measuring the applied mechanical force to lever, input mechanical power to the system in all valve situations is calculated. Mechanical force period is almost fixed and is near 2 seconds and its stroke is 70 cm. Lever velocity and input mechanical power are defined as below:

$$P_{in}(w) = F_{avg}.v \quad (1)$$

$$v(\frac{m}{s}) = \frac{\Delta x}{t} = \frac{0.7}{1} = 0.7(\frac{m}{s}) \quad (2)$$

Where P_{in} is input power (W), F_{avg} is the mean force applied to the lever (N), v is lever velocity $(^{m}/_{s})$, Δx is lever stroke (m) and t is time (s).

4.2. Hydraulic (hydro) power

As mentioned, with flowing of hydraulic oil through various elements of the hydraulic circuit, pressure drop and dissipation occur; however, with the passage of hydraulic oil through the HM, there is a huge difference in pressure, of which only part of the potential generated is used to generate power, and the rest is wasted in the form of dissipation. So the produced power can be obtained by Eq.(3) [16]:

$$P_{HM}(w) = Q * \Delta p * \frac{\eta_t}{600} * 1000 \quad (3)$$

Q is HM flow rate $(^{l}/_{min})$, Δp is HM pressure difference (bar), and η_t is HM efficiency. Pressure difference is recorded during the test and HM flow rate can be achieved by rotational velocity of the HM shaft, as follows.

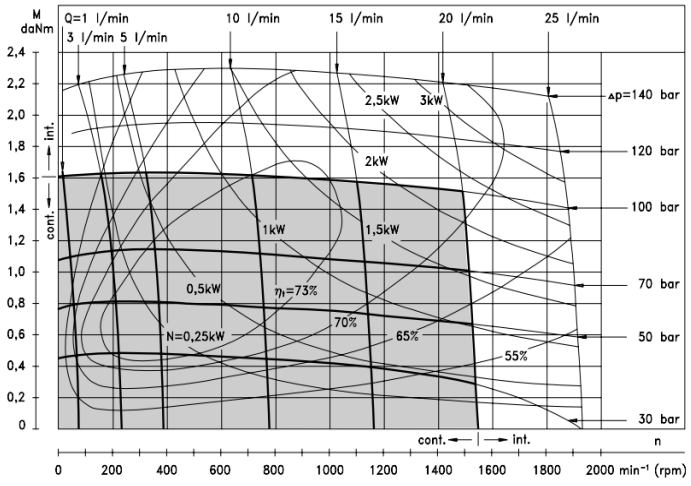

Figure 14. Hydro motor performance diagram [17]

$$Q\left(^{l}/_{min}\right) = \frac{\omega(RPM) * V_g(cm^3)}{1000} \quad (4)$$

V_g is HM displacement (fixed value) and ω is rotational velocity of the HM shaft. By using flow rate and pressure difference, the efficiency of the hydro motor can be read on its performance diagram (Figure 14).

4.3. Electrical power

By measuring electric voltage and current, generator power as output of the system can be written as Eq.(5):

$$P_G(w) = V.I \quad (5)$$

I is current intensity (A) an V is electric voltage (V). To display the trend of electrical power variations per control valve position change, curve fitting is used. A pair of sample for 34 and 50 ohms resistance are presented in Figure 15.

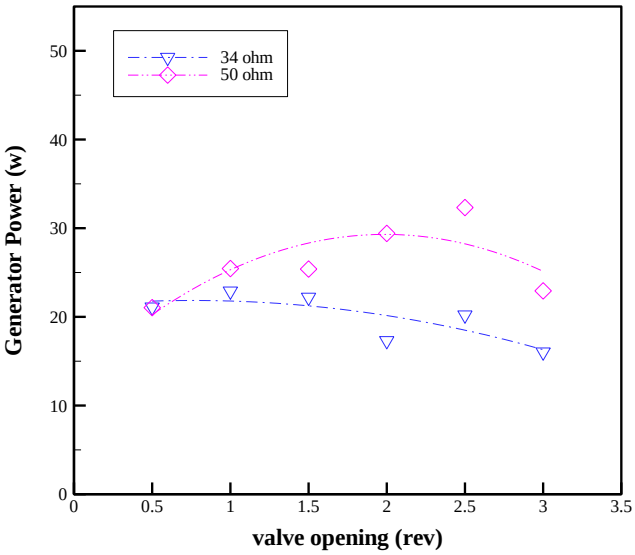

Figure 15. Curve fitting on calculated electrical power

4.4. Wasted power

Wasted power is actually the power that generator cannot convert it to output electricity. For better comparison, the parameter GDP is defined as dissipated power percentage (Generator Damping Percentage) (Eq.(6)).

$$GDP = (1 - \frac{P_G}{P_{HM}}) * 100 \quad (6)$$

In the previous equation, P_G is generator output power and P_{HM} is HM output power. Figure 16 illustrates dissipated power percentage for generator. In this figure, experimental data are fitted by quadratic polynomial curve. Comparing damping percentage in these two cases shows that high resistances wastes less power.

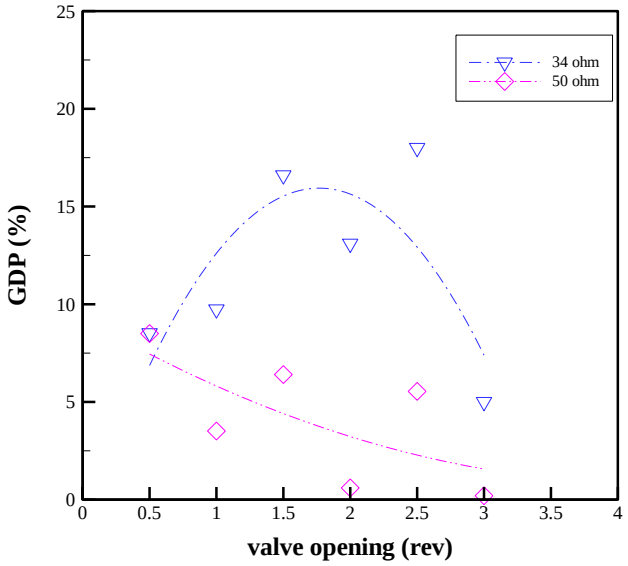

Figure 16. Dissipated power percentage for Generator

4.5. System efficiency

According to mechanical and electrical power (input and output power, respectively), whole WEC system efficiency (including PTO and the absorber efficiency) can be calculated as Eq.(7):

$$\eta_{WEC} = \frac{P_G}{P_{in}} * 100 \qquad (7)$$

P_{in} is input mechanical power. It is worth noting that for displaying the WEC efficiency trend, curve fitting is used. A sample of result for 34 and 50 ohms resistance can be seen in Figure 17.

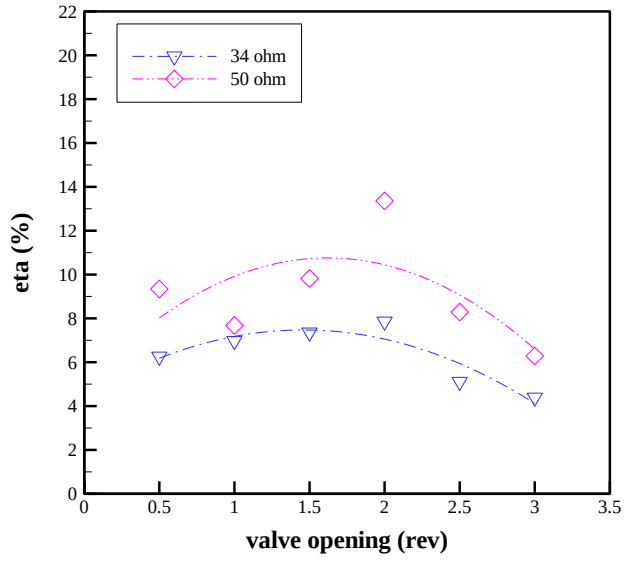

Figure 17. WEC system efficiency and related quadratic curve fitting for 2 different load values

5. Results and Discussion

Due to calculation procedure, the results are provided herein, in order to determine the best valve opening position and also the most suitable value of resistance. In this regard, to calculate the total efficiency of PTO, first, input and then, output values (mechanical and electrical powers, respectively) are calculated. Furthermore, for more detailed description, related diagrams to obtained results will be provided.

Figure 18 represents the results of input mechanical power in all control valve positions. As can be seen, applied mechanical force to the lever is not equal in all test conditions; but it should be reminded that the force period and course are always constant which are equal to 2 seconds and 70 cm, respectively. As a result, the stable input power has different values.

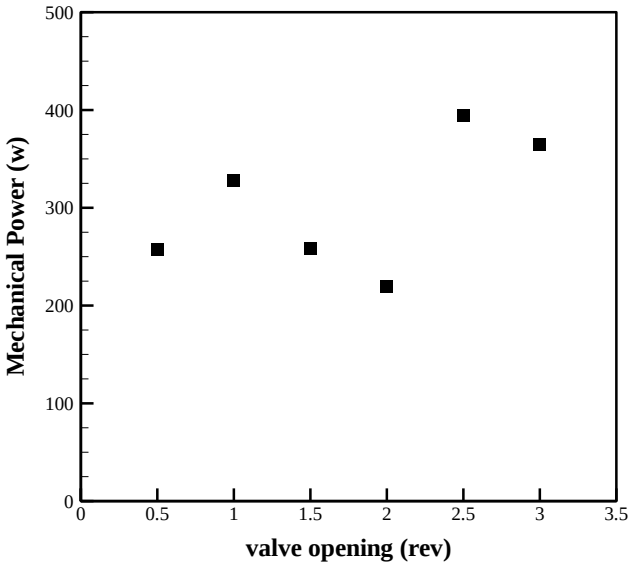

Figure 18. Input mechanical power per valve opening positions

Figure 19 displays generator electrical power in different control valve positions and loads. Considering this figure, output power almost enhances by increasing the resistance of rheostat. Nevertheless, in 22, 50, and 54.8 ohms, the extremums can be seen.

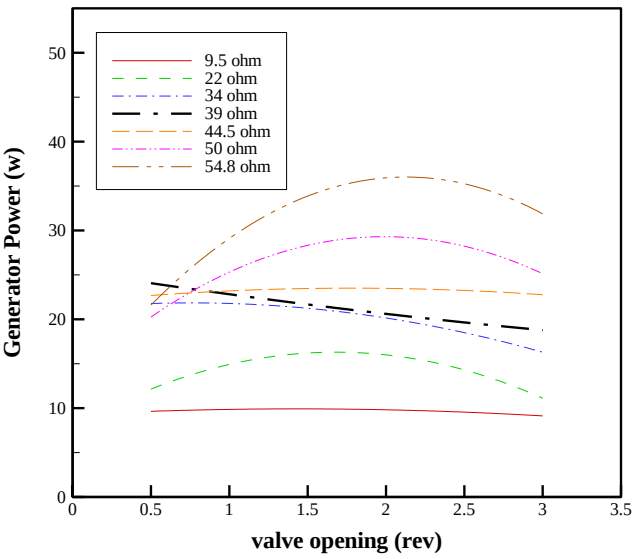

Figure 19. Output power of generator for all valve opening positions in various resistant loads

By determining input and output power to the system, WEC efficiency is presented in the form of Figure 20. Efficiency of WEC system in six control valve positions and seven different resistant load values are drawn using interpolation curves. As can be seen, by increasing the resistance, efficiency increases, too. The maximum system efficiency happens in high resistances and in 2 rev. valve opening. This trend applies to3 different values of rheostat. In fact, the diagram shows that, a maximum point exists between the two positions 1.5 and 2 rev; but, this maximum in low resistance happens between 1 and 1.5 rev. After position 2.5 rev. and in 3 rev, a severe drop can be seen. This result is true for all 7 resistance, so the existence of an extremum point has occurred according to the initial assumption.

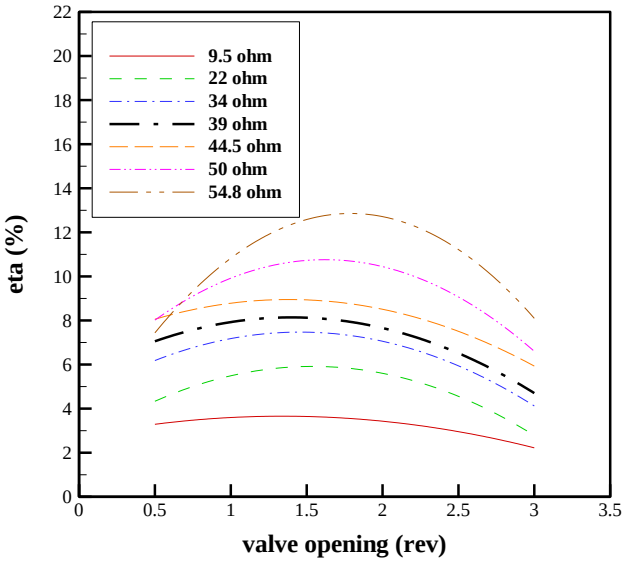

Figure 20. System efficiency curve fitting per all valve opening positions in 7 resistant loads

Figure 20 clearly shows the importance of control valve and rheostat setting. In the position 2 rev, variation of rheostat value from 9.5 to 54.8 ohms, increases the efficiency up to 250%. Also, changes in this parameter in other situations can lead to 170% increment (at least) in the efficiency. In all 7 different resistances, efficiency in 2 rev. valve opening position shows an enhancement of at least 6% and at most 36% compared to its previous position (1.5 rev. valve opening). Also, efficiency of this position, in comparison to the next position (2.5 rev. valve opening) increases at least 28% and at most 73%. Average efficiency enhancement is about 40% over all tests by changing the valve position. It is clear that the changes in the efficiency of this particular position compared to the 0.5 and 3 rev. positions are more than above values.

Figure 21 shows the effect of resistance changes on efficiency better. As noted before, system efficiency increases by increasing the resistant load. The important point in this diagram is that the diagrams of the positions of 0.5, 1, 1.5 and 3 openings are approaching their maximum. Due to this observation, it can be predicted that an extremum point exists for each specific situation of the PTO system. But this statement cannot be seen for 1.5 and 2 rev. positions; means that extremum point for these positions occur in higher loads while other situations are very close to extreme point and after reaching the maximum, efficiency decreases. High efficiency value of position 2 rev. among all valve positions can be observed clearly.

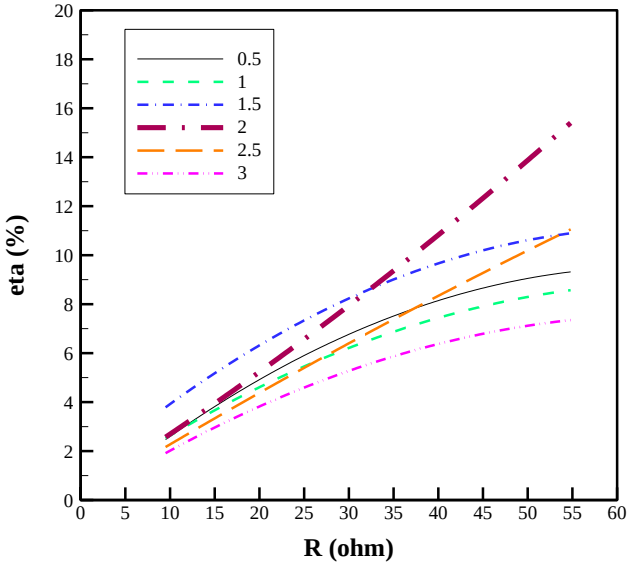

Figure 21. System efficiency per load changes

Pursuant to Figure 21, in the maximum resistance value, efficiency is declined in positions of 0.5 and 1 rev. and then is rised in 2 rev. situation; again from position of 2 rev. to the position of 3 rev, reduction trend can be seen. Actually, the figure shows the contrast between 1.5 and 2 rev. positions. Before 35 ohms resistances, 1.5 rev. valve opening provides more efficiency; and then after 35ohms, the most efficiency belongs to 2 rev. valve opening. As well, Figure 20 confirms this result.

As it is clear in Figure 22, at low resistant loads, generator power dissipation is so high; reaches 45% in 9.5 ohms resistance. Also, it can be seen that the dissipation enhances by increasing the resistance; until it reaches below 5% in 54.8 ohms. Due to previous results, maximum power production and efficiency and of course the least power dissipation are occurred in 54.8 ohm resistance.

According to the presented results, the position of 2 rev. valve opening with a resistance of 54.8 ohms gives the best response to the defined inputs. For better analysis, the output voltage and current diagrams as well as the output power are presented for this optimal position (Figures 23 and 24); In this case, the maximum power generated is 31 watts.

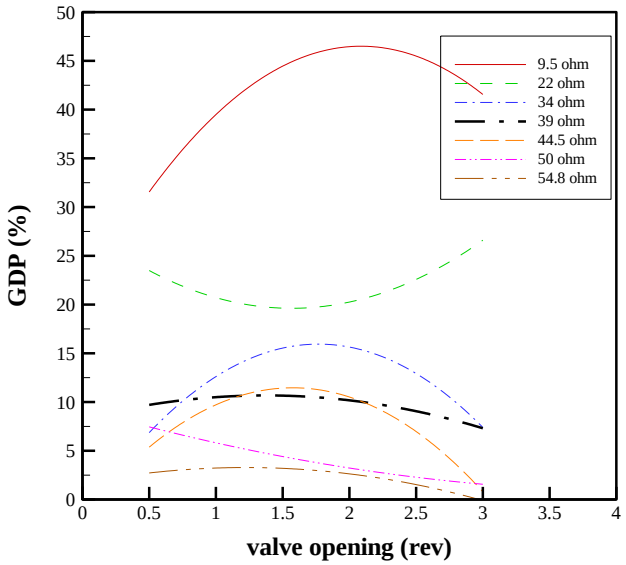

Figure 22. Dissipated power percentage per valve opening situations in 7 resistant loads

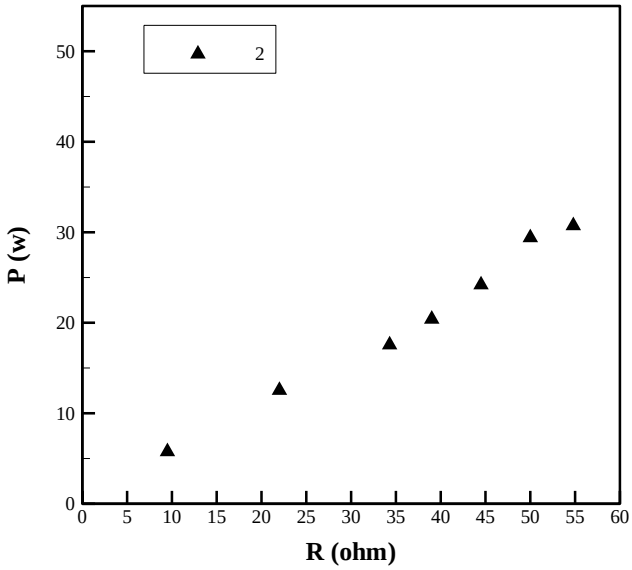

Figure 24. Output power for 2 rev position during test

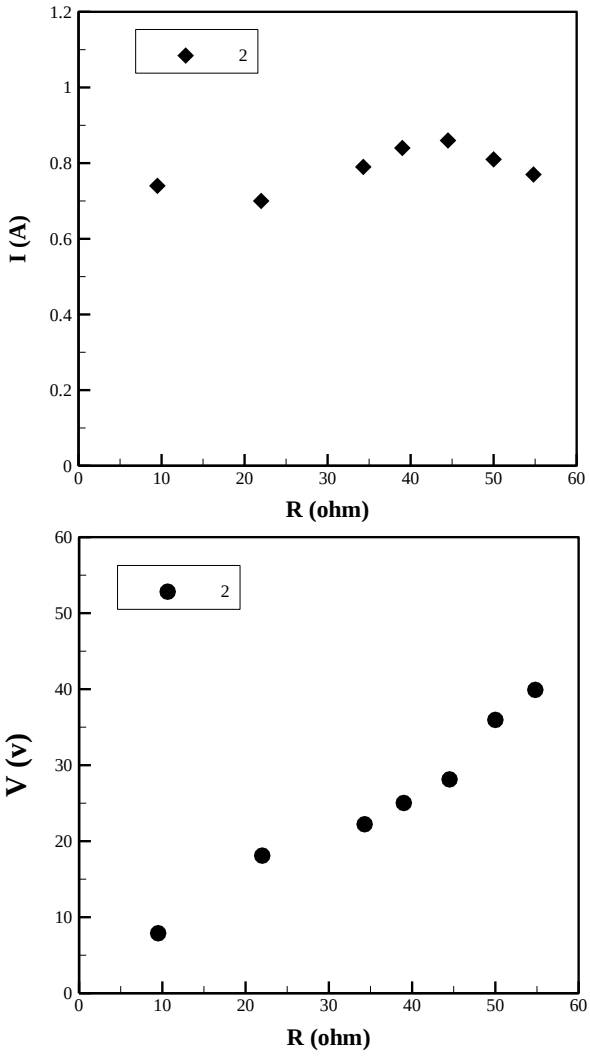

Figure 23. Voltage and current diagrams for 2 rev position during test

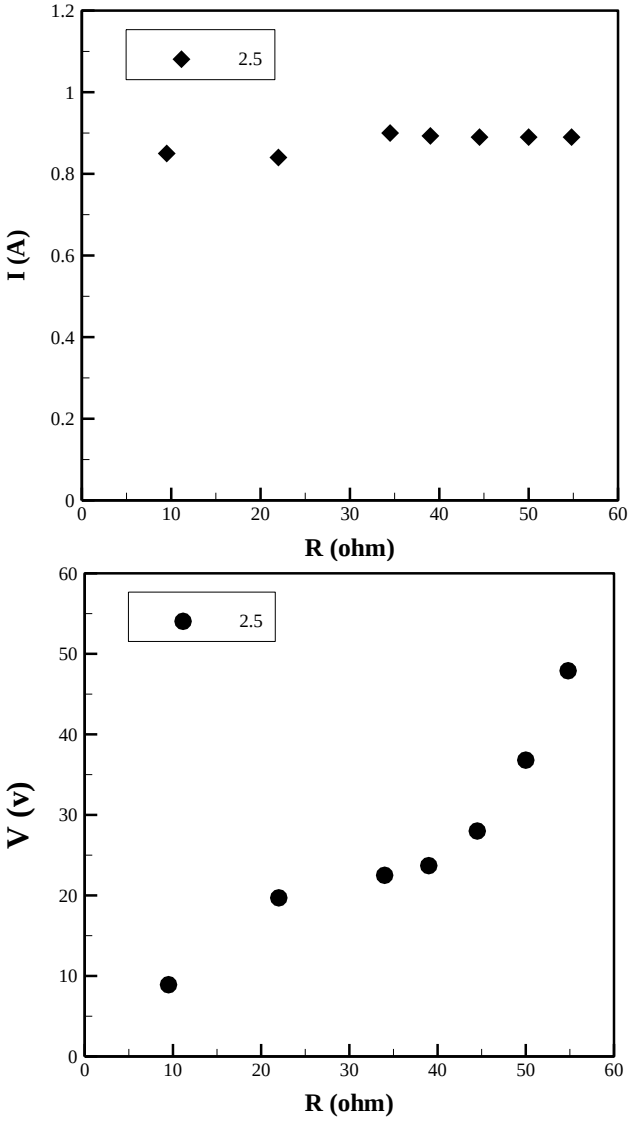

Figure 25. Voltage and current diagrams for 2.5 rev position during test

Figures 25 and 26 show generator output voltage, current, and power in 2.5 rev. valve opening. It is clear that output power rises to more than 42 watts. Produced power in this position is more than others; but about efficiency, 2 rev. valve opening case is higher.

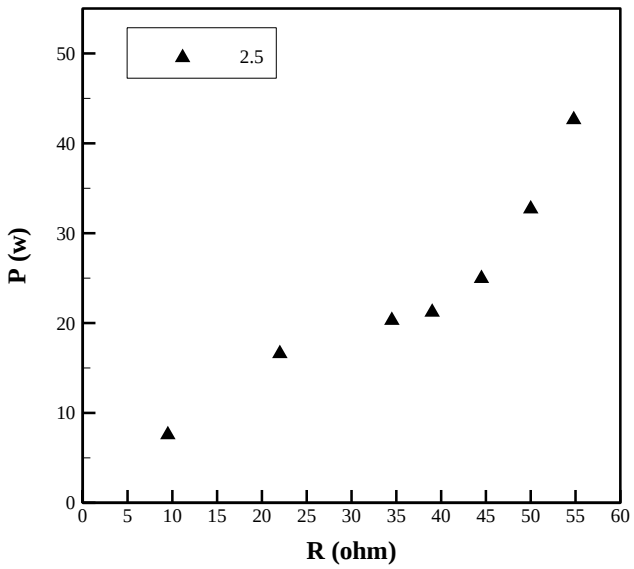

Figure 26. Output power for 2.5 rev position during test

In order to adapt test result to practical situation, it is needed to test the WEC in the wave tank. In this regard, some changes are necessary i.e. a proper buoy and an elongated arm, with an appropriate mechanism transferring wave energy to hydraulic cylinder more efficient. Then Froude similarity is used as follows:

$$\frac{H_2}{H_1} = \alpha_L \quad (8)$$

$$\frac{T_2}{T_1} = {\alpha_L}^2 \quad (9)$$

Here H and T represent wave height and wave period respectively and α_L is a dimension ratio between prototype and actual model.

6. Conclusions

In this investigation, performance of a hydraulic power take-off system in an attenuator wave energy converter named centipede WEC is analyzed experimentally. Dry case experiment condition is provided for the test unit to carry out the defined tests out of the wave tank. For modeling the effect of input wave on hydraulic actuator, an external mechanical force is used. Hydraulic PTO system response to input power is analyzed and evaluated. In this regard, resistance value of rheostat and control valve opening positions as main variables, are described to control WEC system efficiency. The output of the PTO system is evaluated as electrical power proportional to the defined load; also, measured generator voltage and current are analyzed. Significant result are as follows:

- Resistant load variations affect the output power and efficiency dramatically. For instance, according to certain inputs, efficiency improve from 4.2% in 9.5 ohms resistance to 14.7% in 54.8 ohms resistance.
- WEC system efficiency for particular positions like 0.5, 1, 1.5 and 3 rev. valve opening approaches to the maximum of the diagram; means in such conditions, the diagram reach to its peak for a specific resistance. In this condition, increasing resistance to higher values is not beneficial and causes losses and increases costs.
- In all seven resistances, changing control valve opening has a positive effect. In a certain position, maximum value can be achieved; the maximum point for 9.5 to 35 ohms resistances is occurred on 1.5 rev. valve opening and for resistances above 35 ohms is occurred on 2 rev. control valve opening.
- Maximum generator output power can be achieved in 2.5 rev. control valve opening; however, in 2 rev. position, the maximum efficiency is occurred. In implementation plans, this survey can be helpful for reducing costs.

Acknowledgment

The results presented in this article are the outcome of a research project approved by the Supreme Council for Science, Research and Technology (SCSRT). We would like to express our gratitude for the spiritual and funding support of the Mazandaran Provincial Government, the Deputy Governor for Economic Affairs and Resource Development.

List of Symbols

F_{avg}	Average force applied to the lever $[N]$
GDP	Generator Damping Percentage [%]
H_1	Prototype wave height $[m]$
H_2	Real model wave height $[m]$
I	Current $[A]$
P_G	Generator output power $[w]$
P_{HM}	Hydro Motor output power $[w]$
P_{in}	Mechanical inlet power $[w]$
Q	HM flow rate $[{}^{l}/_{min}]$
t	Time $[s]$
T_1	Prototype wave period $[s]$
T_2	Real model wave period $[s]$
v	Averaged velocity of lever $[{}^{m}/_{s}]$

V	Voltage $[V]$
V_g	Hydro motor displacement $[cm^3]$
Δp	Pressure difference $[bar]$
Δx	Stroke $[m]$
ω	HM rotational velocity $[RPM]$
η_{WEC}	Total system efficiency [%]
η_t	HM efficiency [%]
α_L	dimension ratio

9. References

[1] J. Falnes, "A review of wave-energy extraction," *Marine structures*, vol. 20, no. 4, pp. 185-201, 2007.

[2] I. López, J. Andreu, S. Ceballos, I. M. de Alegría, and I. Kortabarria, "Review of wave energy technologies and the necessary power-equipment," *Renewable and sustainable energy reviews*, vol. 27, pp. 413-434, 2013.

[3] M. Den Elzen, A. Admiraal, M. Roelfsema, H. van Soest, A. Hof, and N. Forsell, "Contribution of the G20 economies to the global impact of the Paris agreement climate proposals," *Climatic Change*, vol. 137, no. 3-4, pp. 655-665, 2016.

[4] R. Alamian, R. Shafaghat, and M. Ghasemi, "Experimental evaluation of attenuator WEC in a laboratory wave tank," (in eng), *Journal Of Marine Engineering*, Research Paper vol. 14, no. 28, pp. 1-9, 2019.

[5] M. Negahdari, H. Dalayeli, and M. Moghadas, "modelling and analyzing piont absorber WEC for a cylinderical buoy in heave motion," (in persian), 1394.

[6] P. Yoosefi Khiabani, M. A. Abbaszadeh, A. Khorshid, and M. M. Ettefagh, "Investigation of WaveStar Energy Converter Performance in Caspian Sea Using Regular Wave and Froude-Krylov Force," (in persian), *Journal Of Marine Engineering*, Research Paper vol. 12, no. 23, pp. 45-55, 2016.

[7] R. Waters *et al.*, "Experimental results from sea trials of an offshore wave energy system," *Applied Physics Letters*, vol. 90, no. 3, p. 034105, 2007.

[8] H. Sarlak, M. S. Seif, and M. Abbaspour, "Experimental investigation of offshore wave buoy performance," *Journal of Marine Engineering*, vol. 6, no. 11, pp. 0-0, 2010.

[9] R. Henderson, "Design, simulation, and testing of a novel hydraulic power take-off system for the Pelamis wave energy converter," *Renewable energy*, vol. 31, no. 2, pp. 271-283, 2006.

[10] B. Drew, A. Plummer, and N. Sahinkaya, "A review of wave energy converter technology," vol. 223, ed: Sage Publications Sage UK: London, England, 2009, pp. 887-902.

[11] R. Hansen, T. Andersen, H. Pedersen, and A. Hansen, "Control of a 420 kn discrete displacement cylinder drive for the wavestar wave energy converter," in *ASME/BATH 2014 Symposium on Fluid Power and Motion Control*, 2014: American Society of Mechanical Engineers Digital Collection.

[12] H.-N. Nguyen, G. Sabiron, P. Tona, M. M. Kramer, and E. Vidal Sanchez, "Experimental validation of a nonlinear MPC strategy for a wave energy converter prototype," in *ASME 2016 35th International Conference on Ocean, Offshore and Arctic Engineering*, 2016: American Society of Mechanical Engineers Digital Collection.

[13] M. Lopes, J. Hals, R. Gomes, T. Moan, L. Gato, and A. d. O. Falcão, "Experimental and numerical investigation of non-predictive phase-control strategies for a point-absorbing wave energy converter," *Ocean Engineering*, vol. 36, no. 5, pp. 386-402, 2009.

[14] M. Kramer, L. Marquis, and P. Frigaard, "Performance evaluation of the wavestar prototype," in *Proceedings of the 9th European Wave and Tidal Energy Conference, Southampton, UK*, 2011, pp. 5-9: Citeseer.

[15] R. Alamian, R. Shafaghat, R. Bayani, and A. H. Amouei, "An experimental evaluation of the effects of sea depth, wave energy converter's draft and position of centre of gravity on the performance of a point absorber wave energy converter," *Journal of Marine Engineering & Technology*, vol. 16, no. 2, pp. 70-83, 2017.

[16] "Hydraulic Motors, Variable Displacement," in *HY30-8223/UK*, P. Hannifin, Ed., ed. sweden, 2014.

[17] "HYDRAULIC MOTORS MM," ed.